International Applied Mechanics, Vol. 41, No. 4, 2005

ELASTOPLASTIC DEFORMATION OF A COMPOUND DISK UNDER IMPULSIVE LOADING

V. V. Piskun

UDC 539.374

The small elastoplastic deformation theory and the finite-element method are used to analyze the behavior of a compound disk under axisymmetric impulsive loading. Numerical results are presented, which describe the development of plastic deformation, the effect of hardening and the duration of the loading impulse on the oscillatory elastoplastic deformation of the disk

Keywords: solid of revolution, theory of plasticity, isotropic material, finite elements, impulsive loading, unloading

A method for solving the axisymmetric dynamic problem for isotropic elastoplastic solids of revolution with arbitrary meridional section under impulsive thermomechanical loading was proposed in [11]. The method is based on small elastoplastic deformation theory [1, 2, 8, etc.] and involves the finite-element approximation of unknown displacements in spatial coordinates and finite-difference representation of time derivatives. The nonlinear problem is linearized by the method of variable parameters. In the present paper, this method is extended to compound solids of revolution of finite dimensions. By a compound solid is meant a discretely inhomogeneous solid of revolution whose constituents are solids of revolution. For the entire body and for its parts, there is a common axis of revolution coinciding with the z-axis of a cylindrical coordinate system z, r, φ. The constituents of the body are made of dissimilar isotropic materials characterized by different (real) limit σ–ε relationships and are in perfect mechanical contact with each other.

1. Solution Method. Let the basic unknowns be the axial ($U_z(z, r, t)$) and radial ($U_r(z, r, t)$) displacements. We will use a triangular ring finite element with linear approximation of the displacement vector to partition the meridional section of the solid into triangles by a technique described in [4]. If the meridional section is approximated by N nodes and M triangles with node numbers i, j, and k, then we have the following recurrent formulas of the explicit scheme for computing the displacements at the time $(t + \Delta t)$ in terms of the displacement at the previous times t and $(t - \Delta t)$:

$$u_z^i(t+\Delta t)=2u_z^i(t)-u_z^i(t-\Delta t)-\frac{(\Delta t)^2}{\sum\limits_{m=1}^{M_1} M_m^i}\sum_{m=1}^{M_1}\Big[a_{ii}^{(m)}u_z^i(t)+b_{ii}^{(m)}u_r^i(t)$$

$$+a_{ij}^{(m)}u_z^j(t)+b_{ij}^{(m)}u_r^j(t)+a_{ik}^{(m)}u_z^k(t)+b_{ik}^{(m)}u_r^k(t)+a_{1i}^{(m)}\Big],$$

$$u_r^i(t+\Delta t)=2u_r^i(t)-u_r^i(t-\Delta t)-\frac{(\Delta t)^2}{\sum\limits_{m=1}^{M_1} M_m^i}\sum_{m=1}^{M_1}\Big[c_{ii}^{(m)}u_z^i(t)+d_{ii}^{(m)}u_r^i(t)$$

S. P. Timoshenko Institute of Mechanics, National Academy of Sciences of Ukraine, Kiev. Translated from Prikladnaya Mekhanika, Vol. 41, No. 4, pp. 94–99, April 2005. Original article submitted June 18, 2004.

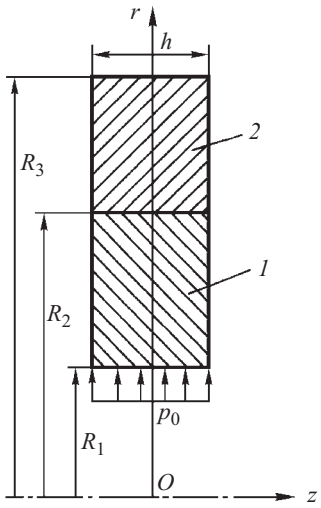

Fig. 1

TABLE 1

ε, %	0	0.20	0.22	0.25	0.30	0.40	0.60	0.90	3.00
σ, MPa	0	140	143	148	154	162	172	180	220
	0	140	145	150	158	170	186	200	260
	0	140	150	160	170	186	214	246	346

TABLE 2

ε, %	0	0.1	0.2	0.3	0.4	0.6	0.8	1.0	1.2
σ, MPa	0	200	292	340	380	440	486	510	522

$$+c_{ij}^{(m)}u_z^j(t)+d_{ij}^{(m)}u_r^j(t)+c_{ik}^{(m)}u_z^k(t)+d_{ik}^{(m)}u_r^k(t)+b_{1i}^{(m)}\Big], \tag{1.1}$$

where the superscript (m) refers to the mth triangular element, M_1 is the number of elements that have the node i, and Δt is the step of integration over time. It should be remembered that $a_{ii}^{(m)}$, ..., $a_{1i}^{(m)}$, $c_{ii}^{(m)}$, ..., $b_{ii}^{(m)}$, and M_m^i appearing in the sums in (1.1) depend on the material properties of the triangular elements around the node i. The quantities with the superscripts i, j, and k correspond to their values at the nodes of an isolated triangular element with nodes i, j, and k. On each time interval, the numerical solution of the elastoplastic problem is obtained by the iterative method of variable parameters. The convergence criterion for the iterative process is the same as that used to solve quasinonstationary elastoplastic problems [5, 7]. Unloading is a linear process. At each step of integration after the first iteration, the conditions of active loading and unloading are tested. To trace the history of the process, the intensity of total shear strain $\Gamma = (0.5e_{ij}e_{ij})^{0.5}$, the intensity of plastic strain $\Gamma_p = (0.5e_{ij}^p e_{ij}^p)^{0.5}$, the components of the plastic-strain tensor, and a parameter specifying the direction of active loading or unloading are stored for each finite element at each time step.

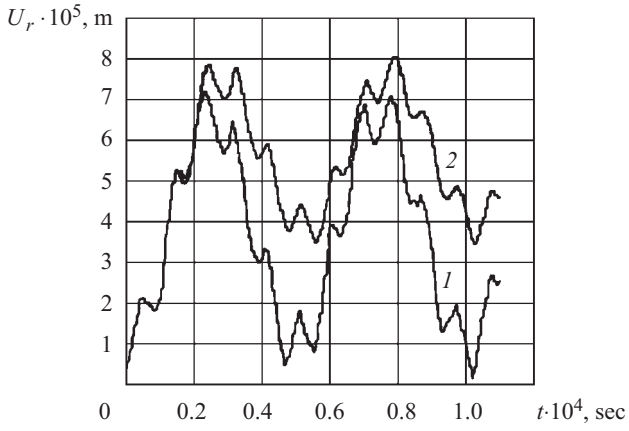

Fig. 2

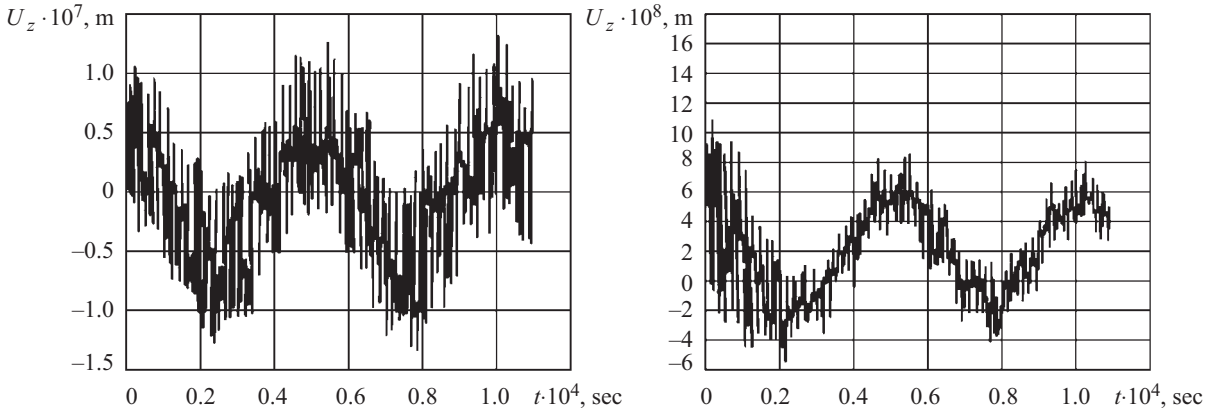

a *b*

Fig. 3

We used this method to study the behavior of a compound disk with a central hole under an impulsive mechanical load causing elastoplastic strains. In what follows, we will discuss the computed results describing the development of plastic strains, the influence of hardening and impulse duration on the oscillatory processes of elastoplastic deformation.

2. Example. We have solved numerically the elastoplastic stress–strain problem for a hollow compound disk whose half the meridional section and loading scheme are shown in Fig. 1. The geometrical parameters of the disk are: outer radius $R_3 = 0.0508$ m, inner radius $R_1 = 0.0254$ m, thickness $h = 0.004$ m, and radius of the cylindrical interface between the constituents $R_2 = 0.0381$ m. The lateral and outer cylindrical surfaces of the disk are free from loads, and the inner cylindrical surface is instantaneously subjected, at $t = 0$, to a uniform surface load $P_0 = 80$ MPa, which remains constant for $t > 0$. Part *1* of the disk (Fig. 1) is made of an aluminum alloy and part *2* of steel. Three limit σ–ε relationships are given in Table 1 for the aluminum alloy and in Table 2 for the steel. The mechanical characteristics of the materials are the following: Poisson's ratio $\nu = 0.3$, Young's modulus $E = 2 \cdot 10^5$ MPa, density $\rho = 8 \cdot 10^3$ kg/m^3 (for the steel) and $\nu = 0.3$, $E = 7 \cdot 10^4$ МПа, and $\rho = 2.82 \cdot 10^3$ kg/m^3 (for the aluminum alloy).

Owing to symmetry, we analyzed just a quarter the meridional section of the disk, specifying symmetry conditions in the plane $z = 0$. The step of integration over time was selected considering both stability conditions and the results of a numerical experiment with mesh refinement in both coordinates and time. The integration step $\Delta t = 0.1 \cdot 10^{-7}$ sec.

The computed results are plotted in Figs. 2–6.

Curves *1* and *2* in Fig. 2 show the time dependence of the radial displacement u_r of a point on the disk surface ($z = 0$) where the external load is applied in the elastic and elastoplastic cases, respectively. For the aluminum alloy, the limit stress–strain relationship in the first row of Table 1 is used. The maximum elastoplastic displacements are larger than the elastic displacements. However, when plastic strains are allowed for, the amplitude of oscillation is much less than in the elastic case.

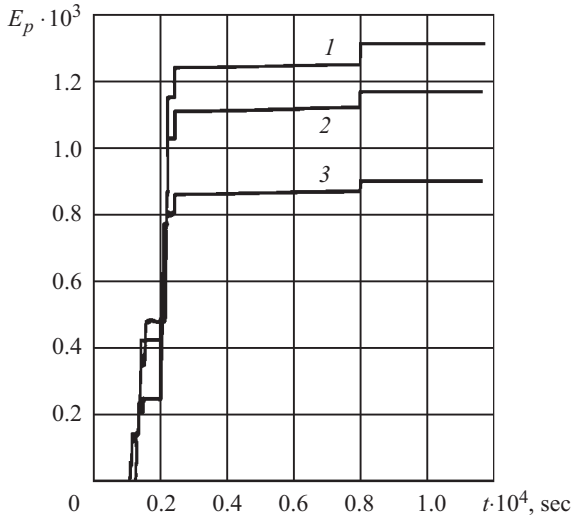

Fig. 4

Figure 3*a*, *b* shows how the axial displacements u_z of points on the inner cylindrical surface at a distance of 0.34 mm from the symmetry plane $z = 0$ vary with time in the elastic and elastoplastic cases, respectively. It can be seen from Fig. 3*a* that the elastic solution leads to a complex oscillatory process of deformation along the disk thickness with almost constant amplitude that is superimposed on the process of radial deformation. The ratio of the frequencies of these two processes is determined by the ratio of the radius of the disk to its half-thickness.

The plastic strains (occurring at $t \geq 0.12 \cdot 10^{-4}$ sec) reduce by half the amplitudes of oscillatory variation in the displacements caused by wave processes along thickness. The maximum elastoplastic displacements along thickness decrease by 30–40%.

Figure 4 shows the accumulation of the intensity of plastic strains $\Gamma_p = (0.5 e_{ij}^p e_{ij}^p)^{0.5}$ with time at a point of the inner cylindrical surface. Lines *1–3* refer to the three limit stress–strain relationships (Table 1) for the aluminum alloy. The value of Γ_p strongly depends on the limit stress–strain relationship. The less the hardening of the material, the greater the intensity of plastic strains Γ_p. Since Γ_p is nondecreasing with time (a linear law of unloading is adopted), it follows from Fig. 4 that the plastic strains accumulate mostly on the time interval $0.12 \cdot 10^{-4} \leq t \leq 0.25 \cdot 10^{-4}$ sec, i.e., until the first maximum of radial displacements (Fig. 2). When the second maximum of displacements occurs at $t = 0.8 \cdot 10^{-4}$ sec, the intensity Γ_p slightly increases. It can also be seen from Fig. 4 that irrespective of the limit stress–strain relationship used (they are characterized by the same limit of proportionality), Γ_p increases at the same time points (steps of curves *1–3* in Fig. 4). Note that the curves have been plotted for the time interval during which an elastic wave travels a distance equal to 20 radii of the disk.

Figure 5 shows how the radial displacements U_r of points on the inner cylindrical surface vary with time in a homogeneous disk made of aluminum alloy (curve *1*) and in a compound disk (curve *2*). The dashed curve refers to a point on the outer cylindrical surface of the compound disk. Comparing curves *1* and *2*, we see that in the compound disk there are waves reflected from the interface of the materials and from the outer cylindrical surface, which changes significantly the displacement pattern, compared with the homogeneous disk. Since the velocities of elastic waves in the aluminum alloy and steel are almost equal ($C_0 = 5000$ m/sec for the steel and $C_0 = 4982$ m/sec for the aluminum alloy) and the interface is equidistant from the inner and outer surfaces, the wave reflected from the interface reaches the inner surface and the elastic wave reaches the outer surface at the same time. This time is the moment of origin of the dash-and-dot curve in Fig. 5 and the moment of the first break of curve *2* for the compound disk. Similar breaks are also observed at later times, and these breaks are more pronounced than for the homogeneous disk.

To ascertain the influence of the impulse duration on the stress–strain state, we have carried out two more computations for two values ($2 \cdot 10^{-5}$ and $2 \cdot 10^{-6}$ sec) of the duration of the load $P = 80$ MPa instantaneously applied to the compound disk at $t = 0$, i.e., the load was instantaneously removed at $t_1 = 2 \cdot 10^{-5}$ and $t_2 = 2 \cdot 10^{-6}$ sec. For the aluminum alloy, the first limit stress–strain relationship (Table 1) was used. The solid curves in Fig. 6 show how the radial displacements of the inner surface

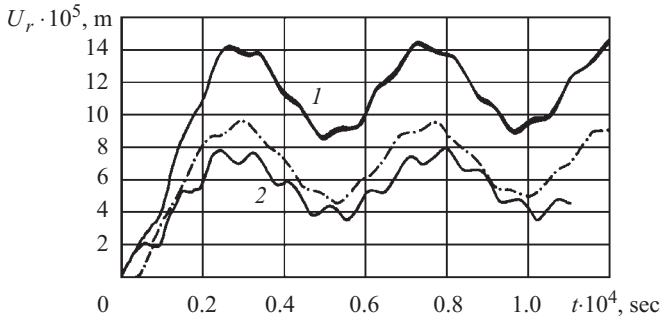

Fig. 5

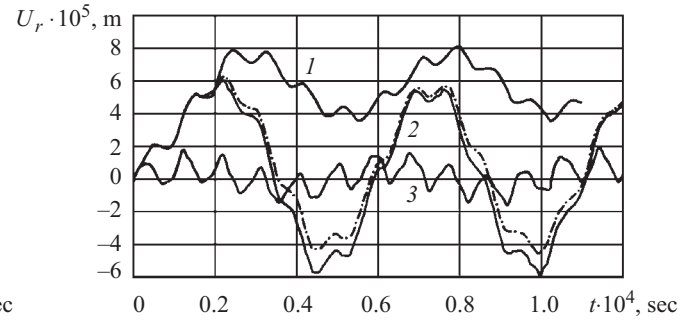

Fig. 6

change with time for constant impulse (curve *1*) and impulses of durations t_1 (curve *2*) and t_2 (curve *3*). The dashed curve represents the elastic solution for a load impulse of duration t_1. It follows from Fig. 6 that the impulse duration strongly influences the behavior of the radial displacements. Note that plastic strains do not occur under impulses of durations t_2. The displacements are positive under constant impulse load (curve *1*) and both positive and negative in the other two cases of load duration.

The above results allow us to conclude that the plastic strains, the interface between dissimilar parts, and impulse duration strongly affect the wave processes in the disk.

In summary, it should be emphasized that the quantitative and qualitative results obtained above are based on small elastoplastic deformation theory that has been justified, both theoretically and experimentally, for processes of loading along rectilinear or nearly rectilinear strain paths [3, 6, 9–11]. It is of interest to validate the obtained results by analyzing paths (processes) of deformation in a compound disk under step impulse loading and to compare them with those produced by the theory of plasticity.

Acknowledgements. The study was partially sponsored by the State Fund for Basic Research of the Ministry of Education and Science of Ukraine (Grant No. 01.07/00010).

REFERENCES

1. A. A. Il'yushin, *Plasticity* [in Russian], Gostekhizdat, Moscow (1948).
2. A. A. Il'yushin, *Plasticity: Fundamentals of General Mathematical Theory* [in Russian], Izd. AN SSSR, Moscow (1963).
3. N. N. Malinin, *Applied Theory of Plasticity and Creep* [in Russian], Mashinostroenie, Moscow (1969).
4. Ya. M. Grigorenko, Yu. N. Shevchenko, et al., *Numerical Methods*, Vol. 11 of the 12-volume series *Mechanics of Composites* [in Russian], A.S.K., Kiev (2002).
5. Yu. N. Shevchenko, M. E. Babeshko, V. V. Piskun, and V. G. Savchenko, *Spatial Problems of Thermoplasticity* [in Russian], Naukova Dumka, Kiev (1980).
6. Yu. N. Shevchenko, M. E. Babeshko, and R. G. Terekhov, *Thermoviscoelastoplastic Deformation of Structural Members* [in Russian], Naukova Dumka, Kiev (1992).
7. Yu. N. Shevchenko, V. V. Piskun, and V. A. Kovalenko, "Elastoplastic state of axisymmetrically loaded laminated bodies of revolution made of isotropic and orthotropic materials," *Int. Appl. Mech*., **28**, No. 1, 25–32 (1992).
8. Yu. N. Shevchenko, *Thermoplasticity under Variable Loading* [in Russian], Naukova Dumka, Kiev (1970).
9. M. E. Babeshko, "Thermoelastoplastic state of flexible laminated shells under axisymmetric loading along various plane paths," *Int. Appl. Mech*., **39**, No. 2, 177–184 (2003).
10. M. E. Babeshko and Yu. N. Shevchenko, "On approximate specification of the functionals of the thermoviscoplastic equations for complex loading along plane paths," *Int. Appl. Mech*., **39**, No. 8, 929–934 (2003).
11. Yu. N. Shevchenko and V. V. Piskun, "Axisymmetric thermoelastoplastic stress state of isotropic solids of revolution under impulsive loading," *Int. Appl. Mech*., **39**, No. 5, 546–555 (2003).